INTERNATIONAL JOURNAL FOR NUMERICAL METHODS IN ENGINEERING
Int. J. Numer. Meth. Engng 2017; **109**:1067–1084
Published online 17 June 2016 in Wiley Online Library (wileyonlinelibrary.com). DOI: 10.1002/nme.5302

Updated Lagrangian/Arbitrary Lagrangian–Eulerian framework for interaction between a compressible neo-Hookean structure and an incompressible fluid

Cornel Marius Murea*,† and Soyibou Sy

Laboratoire de Mathématiques, Informatique et Applications, Université de Haute Alsace, 6, rue des Frères Lumière, 68093 Mulhouse Cedex, France

SUMMARY

We propose a numerical method for a fluid–structure interaction problem. The material of the structure is homogeneous, isotropic, and it can be described by the compressible neo-Hookean constitutive equation, while the fluid is governed by the Navier–Stokes equations. Our study does not use turbulence model. Updated Lagrangian method is used for the structure and fluid equations are written in Arbitrary Lagrangian–Eulerian coordinates. One global moving mesh is employed for the fluid–structure domain, where the fluid–structure interface is an 'interior boundary' of the global mesh. At each time step, we solve a monolithic system of unknown velocity and pressure defined on the global mesh. The continuity of velocity at the interface is automatically satisfied, while the continuity of stress does not appear explicitly in the monolithic fluid–structure system. This method is very fast because at each time step, we solve only one linear system. This linear system was obtained by the linearization of the structure around the previous position in the updated Lagrangian formulation and by the employment of a linear convection term for the fluid. Numerical results are presented. Copyright © 2016 John Wiley & Sons, Ltd.

Received 12 June 2015; Revised 29 February 2016; Accepted 10 May 2016

KEY WORDS: fluid–structure interaction; updated Lagrangian; arbitrary Lagrangian–Eulerian

1. INTRODUCTION

In a fluid–structure interaction problem, the fluid and structure equations are coupled by two boundary conditions: equality of the velocities and equality of the stresses at the fluid–structure interface. This kind of multiphysics problem can be solved numerically using partitioned procedure or monolithic approaches. Partitioned procedure strategy consists in solving separately the fluid and structure sub-problems using an iterative process, in general. This can be performed using fixed-point iterations [1–3], Newton like methods [4–6] or optimization strategies [7–9].

The monolithic approach consists in solving the global fluid–structure system, [10–13]. In the monolithic approach, the boundary conditions at the interface are included in the global system. A drawback is that the coupled fluid–structure system is sometimes ill conditioned and preconditioners are needed [14].

An advantage of the partitioned procedure is that we can use distinct black boxes solvers for the fluid and the structure, respectively. A drawback is that, at each time step, we have to solve many times alternatively fluid and structure sub-problems in order to get the both boundary conditions at the interface. If one of the coupling condition is violated as in the staggered procedures, the numerical scheme can become unstable, as it was shown in [15] for the haemodynamic applications. However, in applications, the staggered procedures are efficient [16, 17].

*Correspondence to: Cornel Marius Murea, Laboratoire de Mathématiques, Informatique et Applications, Université de Haute Alsace, 6, rue des Frères Lumière, 68093 Mulhouse Cedex, France.
†E-mail: cornel.murea@uha.fr

In [18], because a simple structure model, the fluid equations include the structure equation as a Robin boundary condition. In this way, the fluid–structure interaction problem reduces to a fluid problem with moving boundary.

Long time, the staggered procedures were considered to be not suitable for the simulation of incompressible fluid-elastic–structure interaction. Recently, in [19], a new staggered scheme was introduced, which is unconditionally stable for a linear model, and it was successfully applied to two-dimensional and three-dimensional incompressible fluid–structure interaction problems.

In this paper, we use a monolithic strategy for solving the interaction between an incompressible fluid governed by the Navier–Stokes equation with a non-linear elastic structure governed by the compressible neo-Hookean model. Our study does not include turbulence model. A particularity of our approach is using a global moving mesh for the fluid–structure domain, where the fluid–structure interface is an 'interior boundary' of the global mesh. At each time step, we solve a monolithic system of unknown velocity and pressure defined on the global mesh. The continuity of velocity at the interface is automatically satisfied because we use continuous finite elements. The continuity of stress does not appear explicitly in the monolithic fluid–structure system, because of the action and reaction principle. This method is fast compared with a particular partitioned procedure algorithm because at each time step, we solve only one linear system. This linear system was obtained by the linearization of the structure around the previous position in the updated Lagrangian formulation and by the employment of a linear convection term for the fluid.

2. GOVERNING EQUATIONS

We study a two dimensional fluid–structure interaction problem. We denote by Ω_0^S the initial structure domain, and we assume that its boundary admits the decomposition $\partial\Omega_0^S = \Gamma_0^D \cup \Gamma_0^N \cup \Gamma_0$. We suppose that the initial structure domain is undeformed (stress-free). At the time instant t, the structure occupies the domain Ω_t^S bounded by $\partial\Omega_t^S = \Gamma_0^D \cup \Gamma_t^N \cup \Gamma_t$. On the boundary Γ_0^D, we impose zero displacements.

The initial fluid domain Ω_0^F is bounded by: Σ_1 the inlet section, Σ_2 the bottom boundary, Σ_3 the outlet section, and Γ_0 the top boundary (see Figure 1, at the left). The boundary Γ_0 is common of both domains, and it represents the initial position of the fluid–structure interface. At the time instant t, the fluid occupies the domain Ω_t^F bounded by the moving interface Γ_t and by the rigid boundary $\Sigma = \Sigma_1 \cup \Sigma_2 \cup \Sigma_3$ (see Figure 1, at the right).

We denote by $\mathbf{U}^S : \Omega_0^S \times [0, T] \to \mathbb{R}^2$ the displacement of the structure. A particle of the structure whose initial position was the point $\mathbf{X}$ will occupies the position $\mathbf{x} = \mathbf{X} + \mathbf{U}^S(\mathbf{X}, t)$ in the deformed domain Ω_t^S. The gradient of the displacement $\mathbf{U}^S = \left(U_1^S, U_2^S\right)^T$ with respect to the coordinates $\mathbf{X} = (X_1, X_2)^T$ is the matrix

$$\nabla_{\mathbf{X}}\mathbf{U}^S(\mathbf{X}, t) = \begin{pmatrix} \frac{\partial U_1^S}{\partial X_1}(\mathbf{X}, t) & \frac{\partial U_1^S}{\partial X_2}(\mathbf{X}, t) \\ \frac{\partial U_2^S}{\partial X_1}(\mathbf{X}, t) & \frac{\partial U_2^S}{\partial X_2}(\mathbf{X}, t) \end{pmatrix}.$$

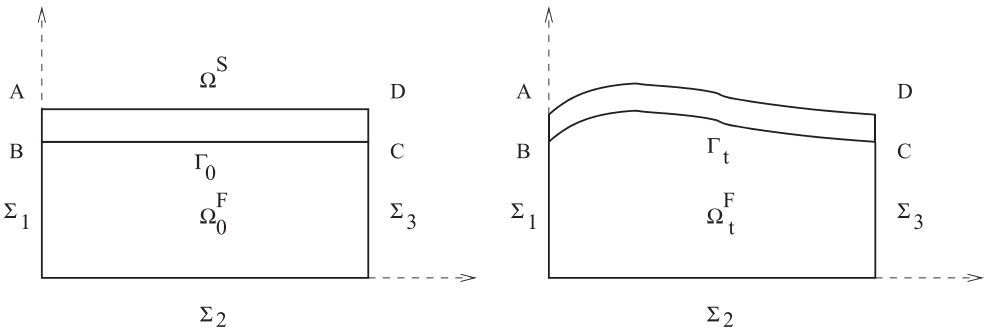

Figure 1. Initial (left) and intermediate (right) geometrical configuration.

DOI: 10.1002/nme

If $\mathbf{A}$ is a square matrix, we denote by $\det \mathbf{A}, tr(A), \mathbf{A}^{-1}, \mathbf{A}^T$ the determinant, the trace, the inverse and the transpose matrix of A, respectively. We write $\mathbf{A}^{-T} = \left(\mathbf{A}^{-1}\right)^T$ and $\operatorname{cof} \mathbf{A} = (\det \mathbf{A}) \left(\mathbf{A}^{-1}\right)^T$ the cofactor matrix of $\mathbf{A}$.

We denote by $\mathbf{F}(\mathbf{X}, t) = \mathbf{I} + \nabla_{\mathbf{X}} \mathbf{U}^S(\mathbf{X}, t)$ the gradient of the deformation, where $\mathbf{I}$ is the unity matrix and we set $J(\mathbf{X}, t) = \det \mathbf{F}(\mathbf{X}, t)$.

The first and the second Piola–Kirchhoff stress tensors are denoted by $\mathbf{\Pi}$ and $\mathbf{\Sigma}$, respectively and the following equality holds $\mathbf{\Pi} = \mathbf{F}\mathbf{\Sigma}$. We suppose that the material of the structure is homogeneous, isotropic and it can be described by the compressible neo-Hookean constitutive equation $\mathbf{\Sigma} = \lambda^S (\ln J)\mathbf{F}^{-1}\mathbf{F}^{-T} + \mu^S \left(\mathbf{I} - \mathbf{F}^{-1}\mathbf{F}^{-T}\right)$, where λ^S, μ^S are the Lamé constants of the linearized theory; see [20] or [21], chapter 5.

We have assumed that the fluid is governed by the Navier–Stokes equations. For each time instant $t \in [0, T]$, we denote the fluid velocity by $\mathbf{v}^F(t) = \left(v_1^F(t), v_2^F(t)\right)^T : \Omega_t^F \to \mathbb{R}^2$ and the fluid pressure by $p^F(t) : \Omega_t^F \to \mathbb{R}$. Let us remark that the fluid domain Ω_t^F depends on the position of the interface Γ_t, which is the image of Γ_0 via the map $\mathbf{X} \to \mathbf{X} + \mathbf{U}^S(\mathbf{X}, t)$.

Let $\epsilon\left(\mathbf{v}^F\right) = \frac{1}{2}\left(\nabla \mathbf{v}^F + \left(\nabla \mathbf{v}^F\right)^T\right)$ be the fluid rate of strain tensor and let $\sigma^F = -p^F \mathbf{I} + 2\mu^S \epsilon\left(\mathbf{v}^F\right)$ be the fluid stress tensor. In order to simplify the notation, we write $\nabla \mathbf{v}^F$ in place of $\nabla_{\mathbf{x}} \mathbf{v}^F$, when the gradients are computed with respect to the Eulerian coordinates $\mathbf{x}$.

We denote by $\dot{\mathbf{U}}^S$ the material time derivative or the total time derivative of the displacement $\mathbf{U}^S$. We have that $\mathbf{V}^S = \dot{\mathbf{U}}^S$ is the velocity and $\ddot{\mathbf{U}}^S = \dot{\mathbf{V}}^S$ is the acceleration of the structure. Using the Lagrangian coordinates, we have $\ddot{\mathbf{U}}^S(\mathbf{X}, t) = \frac{\partial^2 \mathbf{U}^S}{\partial t^2}(\mathbf{X}, t)$ and $\dot{\mathbf{U}}^S = \frac{\partial \mathbf{U}^S}{\partial t}(\mathbf{X}, t)$; see [22], section 2.3. The total time derivative of the fluid velocity using the Eulerian coordinates is $\dot{\mathbf{v}}^F = \frac{\partial \mathbf{v}^F}{\partial t} + (\mathbf{v}^F \cdot \nabla)\mathbf{v}^F$.

The problem is to find the structure displacement $\mathbf{U}^S$, the fluid velocity $\mathbf{v}^F$, and the fluid pressure p^F such that:

$$\rho_0^S(\mathbf{X})\, \ddot{\mathbf{U}}^S(\mathbf{X}, t) - \nabla_{\mathbf{X}} \cdot (\mathbf{F}\mathbf{\Sigma})(\mathbf{X}, t) = \rho_0^S(\mathbf{X})\, \mathbf{g}, \quad \text{in } \Omega_0^S \times (0, T) \tag{1}$$

$$\mathbf{U}^S(\mathbf{X}, t) = 0, \quad \text{on } \Gamma_0^D \times (0, T) \tag{2}$$

$$(\mathbf{F}\mathbf{\Sigma})(\mathbf{X}, t)\, \mathbf{N}^S(\mathbf{X}) = 0, \quad \text{on } \Gamma_0^N \times (0, T) \tag{3}$$

$$\rho^F \left(\frac{\partial \mathbf{v}^F}{\partial t} + (\mathbf{v}^F \cdot \nabla)\mathbf{v}^F\right) - 2\mu^F \nabla \cdot \epsilon\left(\mathbf{v}^F\right) + \nabla\, p^F = \rho^F \mathbf{g}, \forall t \in (0, T), \forall \mathbf{x} \in \Omega_t^F \tag{4}$$

$$\nabla \cdot \mathbf{v}^F = 0, \forall t \in (0, T), \forall \mathbf{x} \in \Omega_t^F \tag{5}$$

$$\sigma^F \mathbf{n}^F = \mathbf{h}_{in}, \quad \text{on } \Sigma_1 \times (0, T) \tag{6}$$

$$\sigma^F \mathbf{n}^F = \mathbf{h}_{out}, \quad \text{on } \Sigma_3 \times (0, T) \tag{7}$$

$$\mathbf{v}^F = 0, \quad \text{on } \Sigma_2 \times (0, T) \tag{8}$$

$$\mathbf{v}^F\left(\mathbf{X} + \mathbf{U}^S(\mathbf{X}, t), t\right) = \frac{\partial \mathbf{U}^S}{\partial t}(\mathbf{X}, t), \text{on} \Gamma_0 \times (0, T) \tag{9}$$

$$\left(\sigma^F \mathbf{n}^F\right)_{\left(\mathbf{X} + \mathbf{U}^S(\mathbf{X}, t), t\right)} \omega(\mathbf{X}, t) = -(\mathbf{F}\mathbf{\Sigma})(\mathbf{X}, t)\, \mathbf{N}^S(\mathbf{X}), \text{ on } \Gamma_0 \times (0, T) \tag{10}$$

$$\mathbf{U}^S(\mathbf{X}, 0) = \mathbf{U}^{S,0}(\mathbf{X}), \text{ in } \Omega_0^S \tag{11}$$

DOI: 10.1002/nme

$$\frac{\partial \mathbf{U}^S}{\partial t}(\mathbf{X},0)=\mathbf{V}^{S,0}(\mathbf{X}),\ \text{in } \Omega_0^S \tag{12}$$

$$\mathbf{v}^F(\mathbf{X},0)=\mathbf{v}^{F,0}(\mathbf{X}),\ \text{in } \Omega_0^F \tag{13}$$

where $\rho_0^S:\Omega_0^S\to\mathbb{R}$ is the initial mass density of the structure, $\mathbf{g}$ is the acceleration of gravity vector and it is assumed to be constant, $\mathbf{N}^S$ is the unit outer normal vector along the boundary $\partial\Omega_0^S$, $\rho^F>0$ and $\mu^F>0$ are constants and its represent the mass density and the viscosity of the fluid, $\mathbf{h}_{in}$ and $\mathbf{h}_{out}$ are prescribed boundary stress, $\mathbf{n}^F$ is the unit outer normal vector along the boundary $\partial\Omega_t^F$. The factor ω appearing in the left-hand side of (10) is defined by $\omega(\mathbf{X},t)=\left\|\text{cof}\ (\mathbf{F})\,\mathbf{N}^S\right\|_{\mathbb{R}^2}=\left\|J\mathrm{F}^{-T}\mathbf{N}^S\right\|_{\mathbb{R}^2}$. We have the identity; see [23], for example,

$$\int_{\Gamma_t}\left(\sigma^F\mathbf{n}^F\right)_{(s,t)}ds=\int_{\Gamma_0}\left(\sigma^F\mathbf{n}^F\right)_{\left(S+\mathbf{U}^S(S,t),t\right)}\omega(S,t)\,dS.$$

For the structure Equations (1)–(3), we have used the Lagrangian coordinates, while for the fluid, Equations (4)–(8), the Eulerian coordinates have been used. The Equations (9) and (10) represent the continuity of velocity and of stress at the interface, respectively. Initial conditions are given by (11)–(13).

The governing equations for fluid–structure interaction are (1)–(13).

3. STRUCTURE APPROXIMATION USING THE TOTAL LAGRANGIAN FRAMEWORK

Usually, the structure equations are solved in the total Lagrangian framework. Let us recall that $\mathbf{V}^S$ is the velocity of the structure in the Lagrangian coordinates. The Equation (1) is equivalent to

$$\rho_0^S(\mathbf{X})\,\dot{\mathbf{V}}^S(\mathbf{X},t)-\nabla_{\mathbf{X}}\cdot(\mathbf{F}\boldsymbol{\Sigma})\left(\mathbf{U}^S\right)(\mathbf{X},t)=\rho_0^S(\mathbf{X})\,\mathbf{g},\quad \text{in } \Omega_0^S\times(0,T) \tag{14}$$

$$\dot{\mathbf{U}}^S(\mathbf{X},t)=\mathbf{V}^S(\mathbf{X},t),\quad \text{in } \Omega_0^S\times(0,T). \tag{15}$$

Let $N\in\mathbb{N}^*$ be the number of time steps and $\Delta t=T/N$ the time step. We set $t_n=n\Delta t$ for $n=0,1,\ldots,N$. Let $\mathbf{V}^{S,n}(\mathbf{X})$ and $\mathbf{U}^{S,n}(\mathbf{X})$ be approximations of $\mathbf{V}^S(\mathbf{X},t_n)$ and $\mathbf{U}^S(\mathbf{X},t_n)$. We also use the following notations

$$\mathbf{F}^n=\mathbf{I}+\nabla_{\mathbf{X}}\mathbf{U}^{S,n},\quad \boldsymbol{\Sigma}^n=\lambda^S(\ln J^n)\,(\mathbf{F}^n)^{-1}(\mathbf{F}^n)^{-T}+\mu^S\left(\mathbf{I}-(\mathbf{F}^n)^{-1}(\mathbf{F}^n)^{-T}\right),\ n\geqslant 0.$$

The system (14)–(15) will be approached by the implicit Euler scheme

$$\rho_0^S(\mathbf{X})\,\frac{\mathbf{V}^{S,n+1}(\mathbf{X})-\mathbf{V}^{S,n}(\mathbf{X})}{\Delta t}-\nabla_{\mathbf{X}}\cdot\left(\mathbf{F}^{n+1}\boldsymbol{\Sigma}^{n+1}\right)(\mathbf{X})=\rho_0^S(\mathbf{X})\,\mathbf{g},\ \text{in } \Omega_0^S \tag{16}$$

$$\frac{\mathbf{U}^{S,n+1}(\mathbf{X})-\mathbf{U}^{S,n}(\mathbf{X})}{\Delta t}=\mathbf{V}^{S,n+1}(\mathbf{X}),\ \text{in } \Omega_0^S \tag{17}$$

From (17), we get $\mathbf{F}^{n+1}=\mathbf{F}^n+\Delta t\nabla_{\mathbf{X}}\mathbf{V}^{S,n+1}$, and consequently, $\mathbf{F}^{n+1}$ and $\boldsymbol{\Sigma}^{n+1}$ depend on the velocity $\mathbf{V}^{S,n+1}$ but not in the displacement $\mathbf{U}^{S,n+1}$. In other word, we have eliminated the unknown displacement, and we have now an equation of unknown $\mathbf{V}^{S,n+1}$.

The weak form of the Equation (16) is: find $\mathbf{V}^{S,n+1}:\Omega_0^S\to\mathbb{R}^2$, $\mathbf{V}^{S,n+1}=0$ on Γ_0^D, such that

$$\begin{aligned}&\int_{\Omega_0^S}\rho_0^S\frac{\mathbf{V}^{S,n+1}-\mathbf{V}^{S,n}}{\Delta t}\cdot\mathbf{W}^S\,d\mathbf{X}+\int_{\Omega_0^S}\mathbf{F}^{n+1}\boldsymbol{\Sigma}^{n+1}:\nabla_{\mathbf{X}}\mathbf{W}^S\,d\mathbf{X}\\&\quad=\int_{\Omega_0^S}\rho_0^S\mathbf{g}\cdot\mathbf{W}^S\,d\mathbf{X}+\int_{\Gamma_0}\mathbf{F}^{n+1}\boldsymbol{\Sigma}^{n+1}\mathbf{N}^S\cdot\mathbf{W}^S\,dS\end{aligned} \tag{18}$$

DOI: 10.1002/nme

for all $\mathbf{W}^S : \Omega_0^S \to \mathbb{R}^2$, $\mathbf{W}^S = 0$ on Γ_0^D. For instant, we have assumed that the forces $\mathbf{F}^{n+1}\boldsymbol{\Sigma}^{n+1}\mathbf{N}^S$ on the interface Γ_0 are known.

4. STRUCTURE APPROXIMATION USING THE UPDATED LAGRANGIAN FRAMEWORK

We rewrite the structure equations in the updated Lagrangian framework, and we will see in the following section that the boundary conditions at the fluid–structure interface will be easily handled.

We denote by Ω_n^S the image of Ω_0^S via the map $\mathbf{X} \to \mathbf{X} + \mathbf{U}^{S,n}(\mathbf{X})$, and we set $\widehat{\Omega}^S = \Omega_n^S$ the computational domain for the structure.

The map from Ω_0^S to Ω_{n+1}^S defined by $\mathbf{X} \to \mathbf{x} = \mathbf{X} + \mathbf{U}^{S,n+1}(\mathbf{X})$ is the composition of the map from Ω_0^S to $\widehat{\Omega}^S$ defined by $\mathbf{X} \to \hat{\mathbf{x}} = \mathbf{X} + \mathbf{U}^{S,n}(\mathbf{X})$ with the map from $\widehat{\Omega}^S$ to Ω_{n+1}^S defined by

$$\hat{\mathbf{x}} \to \mathbf{x} = \hat{\mathbf{x}} + \mathbf{U}^{S,n+1}(\mathbf{X}) - \mathbf{U}^{S,n}(\mathbf{X}) = \hat{\mathbf{x}} + \widehat{\mathbf{u}}(\hat{\mathbf{x}}).$$

With the notations $\widehat{\mathbf{F}} = \mathbf{I} + \nabla_{\hat{\mathbf{x}}}\widehat{\mathbf{u}}$ and $\widehat{J} = \det\widehat{\mathbf{F}}$, $J^n = \det\mathbf{F}^n$, we obtain

$$\mathbf{F}^{n+1}(\mathbf{X}) = \widehat{\mathbf{F}}(\hat{\mathbf{x}})\,\mathbf{F}^n(\mathbf{X}), \quad J^{n+1}(\mathbf{X}) = \widehat{J}(\hat{\mathbf{x}})\,J^n(\mathbf{X}). \tag{19}$$

The relation between the Cauchy stress tensor of the structure σ^S and the second Piola–Kirchhoff stress tensor $\boldsymbol{\Sigma}$ is the following $\sigma^S(\mathbf{x},t) = \left(\frac{1}{J}\mathbf{F}\boldsymbol{\Sigma}\mathbf{F}^T\right)(\mathbf{X},t)$, where $\mathbf{x} = \mathbf{X} + \mathbf{U}^S(\mathbf{X},t)$. For the neo-Hoohean material, $\sigma^S(\mathbf{x},t)$ has the form $\frac{1}{J}\lambda^S(\ln J)\mathbf{I} + \frac{1}{J}\mu^S\left(\mathbf{F}\mathbf{F}^T - \mathbf{I}\right)$.

The mass conservation assumption gives $\rho^S(\mathbf{x},t) = \frac{\rho_0^S(\mathbf{X})}{J(\mathbf{X},t)}$, where $\rho^S(\mathbf{x},t)$ is the mass density of the structure in the Eulerian framework.

For the semi-discrete scheme, we use the notations

$$\sigma^{S,n+1}(\mathbf{x}) = \left(\frac{1}{J^{n+1}}\mathbf{F}^{\mathbf{n+1}}\boldsymbol{\Sigma}^{n+1}\left(\mathbf{F}^{n+1}\right)^T\right)(\mathbf{X}), \quad \mathbf{x} = \mathbf{X} + \mathbf{U}^{S,n+1}(\mathbf{X})$$

and $\rho^{S,n}(\hat{\mathbf{x}}) = \frac{\rho_0^S(\mathbf{X})}{J^n(\mathbf{X})}$, $\hat{\mathbf{x}} = \mathbf{X} + \mathbf{U}^{S,n}(\mathbf{X})$.

Let us introduce $\widehat{\mathbf{v}}^{S,n+1} : \widehat{\Omega}^S \to \mathbb{R}^2$ and $\mathbf{v}^{S,n} : \widehat{\Omega}^S \to \mathbb{R}^2$ defined by $\widehat{\mathbf{v}}^{S,n+1}(\hat{\mathbf{x}}) = \mathbf{V}^{S,n+1}(\mathbf{X})$ and $\mathbf{v}^{S,n}(\hat{\mathbf{x}}) = \mathbf{V}^{S,n}(\mathbf{X})$. Also, for $\mathbf{W}^S : \Omega_0^S \to \mathbb{R}^2$, we define $\widehat{\mathbf{w}}^S : \widehat{\Omega}^S \to \mathbb{R}^2$ and $\mathbf{w}^S : \Omega_{n+1}^S \to \mathbb{R}^2$ by $\widehat{\mathbf{w}}^S(\hat{\mathbf{x}}) = \mathbf{w}^S(\mathbf{x}) = \mathbf{W}^S(\mathbf{X})$.

Now, we rewrite the Equation (18) over the domain $\widehat{\Omega}^S$. For the first term of (18), we get

$$\int_{\Omega_0^S} \rho_0^S \frac{\mathbf{V}^{S,n+1} - \mathbf{V}^{S,n}}{\Delta t} \cdot \mathbf{W}^S\, d\mathbf{X} = \int_{\widehat{\Omega}^S} \rho^{S,n} \frac{\widehat{\mathbf{v}}^{S,n+1} - \mathbf{v}^{S,n}}{\Delta t} \cdot \widehat{\mathbf{w}}^S\, d\hat{\mathbf{x}}$$

and similarly

$$\int_{\Omega_0^S} \rho_0^S \mathbf{g} \cdot \mathbf{W}^S\, d\mathbf{X} = \int_{\widehat{\Omega}^S} \rho^{S,n} \mathbf{g} \cdot \widehat{\mathbf{w}}^S\, d\hat{\mathbf{x}}.$$

Using the identity $\left(\nabla\mathbf{w}^S(\mathbf{x})\right)\mathbf{F}^{n+1}(\mathbf{X}) = \nabla_{\mathbf{X}}\mathbf{W}^S(\mathbf{X})$ and the definition of $\sigma^{S,n+1}$, we get

$$\int_{\Omega_0^S} \mathbf{F}^{n+1}\boldsymbol{\Sigma}^{n+1} : \nabla_{\mathbf{X}}\mathbf{W}^S\, d\mathbf{X} = \int_{\Omega_{n+1}^S} \sigma^{S,n+1} : \nabla\mathbf{w}^S\, d\mathbf{x}.$$

Details about this kind of transformation could be found in [23], chapter 1.2.

In order to write the aforementioned integral over the domain $\widehat{\Omega}^S$, let us introduce the tensor

$$\widehat{\boldsymbol{\Sigma}}(\hat{\mathbf{x}}) = \widehat{J}(\hat{\mathbf{x}})\,\widehat{\mathbf{F}}^{-1}(\hat{\mathbf{x}})\,\sigma^{S,n+1}(\mathbf{x})\,\widehat{\mathbf{F}}^{-T}(\hat{\mathbf{x}}). \tag{20}$$

DOI: 10.1002/nme

Because $\left(\nabla \mathbf{w}^S(\mathbf{x})\right)\widehat{\mathbf{F}}(\hat{\mathbf{x}}) = \nabla_{\hat{\mathbf{x}}}\widehat{\mathbf{w}}^S(\hat{\mathbf{x}})$, see [23], chapter 1.2 and taking into account (20), we get

$$\int_{\Omega_{n+1}^S} \sigma^{S,n+1} : \nabla \mathbf{w}^S \, d\mathbf{x} = \int_{\widehat{\Omega}^S} \widehat{\mathbf{F}}\widehat{\mathbf{\Sigma}} : \nabla_{\hat{\mathbf{x}}}\widehat{\mathbf{w}}^S \, d\hat{\mathbf{x}}.$$

Using the identity $\widehat{\mathbf{u}}(\hat{\mathbf{x}}) = \mathbf{U}^{S,n+1}(\mathbf{X}) - \mathbf{U}^{S,n}(\mathbf{X}) = \Delta t \, \mathbf{V}^{S,n+1}(\mathbf{X}) = \Delta t \, \widehat{\mathbf{v}}^{S,n+1}(\hat{\mathbf{x}})$, we obtain

$$\widehat{\mathbf{F}} = \mathbf{I} + \Delta t \nabla_{\hat{\mathbf{x}}}\widehat{\mathbf{v}}^{S,n+1}. \tag{21}$$

For the neo-Hookean material, we have $\sigma^{S,n+1} = \frac{\lambda^S}{J^{n+1}}(\ln J^{n+1})\mathbf{I} + \frac{\mu^S}{J^{n+1}}\left(\mathbf{F}^{n+1}\left(\mathbf{F}^{n+1}\right)^T - \mathbf{I}\right)$ and using (19), it follows that

$$\begin{aligned}
\widehat{\mathbf{\Sigma}} &= \widehat{J}\widehat{\mathbf{F}}^{-1}\frac{\lambda^S}{J^{n+1}}(\ln J^{n+1})\widehat{\mathbf{F}}^{-T} + \widehat{J}\widehat{\mathbf{F}}^{-1}\frac{\mu^S}{J^{n+1}}\left(\mathbf{F}^{n+1}\left(\mathbf{F}^{n+1}\right)^T - \mathbf{I}\right)\widehat{\mathbf{F}}^{-T} \\
&= \widehat{J}\frac{\lambda^S}{\widehat{J}J^n}\left(\ln J^n + \ln \widehat{J}\right)\widehat{\mathbf{F}}^{-1}\widehat{\mathbf{F}}^{-T} + \widehat{J}\widehat{\mathbf{F}}^{-1}\frac{\mu^S}{\widehat{J}J^n}\left(\widehat{\mathbf{F}}\mathbf{F}^n\left(\widehat{\mathbf{F}}\mathbf{F}^n\right)^T - \mathbf{I}\right)\widehat{\mathbf{F}}^{-T} \\
&= \frac{\lambda^S}{J^n}\left(\ln J^n + \ln \widehat{J}\right)\widehat{\mathbf{F}}^{-1}\widehat{\mathbf{F}}^{-T} + \frac{\mu^S}{J^n}\left(\mathbf{F}^n(\mathbf{F}^n)^T - \widehat{\mathbf{F}}^{-1}\widehat{\mathbf{F}}^{-T}\right).
\end{aligned} \tag{22}$$

Let us remark that $\widehat{\mathbf{F}}$ depends only on $\widehat{\mathbf{v}}^{S,n+1}$, see (21) and $\widehat{\mathbf{\Sigma}}$ depends on $\widehat{\mathbf{v}}^{S,n+1}$ and $\mathbf{F}^n(\mathbf{X})$, see (22).

Now, it is possible to present the updated Lagrangian version of (18). Knowing $\mathbf{U}^{S,n} : \Omega_0^S \to \mathbb{R}^2$, $\widehat{\Omega}^S = \Omega_n^S$ and $\mathbf{v}^{S,n} : \widehat{\Omega}^S \to \mathbb{R}^2$, we try to find $\widehat{\mathbf{v}}^{S,n+1} : \widehat{\Omega}^S \to \mathbb{R}^2$, $\widehat{\mathbf{v}}^{S,n+1} = 0$ on Γ_0^D such that

$$\begin{aligned}
&\int_{\widehat{\Omega}^S} \rho^{S,n}\frac{\widehat{\mathbf{v}}^{S,n+1} - \mathbf{v}^{S,n}}{\Delta t} \cdot \widehat{\mathbf{w}}^S \, d\hat{\mathbf{x}} + \int_{\widehat{\Omega}^S} \widehat{\mathbf{F}}\widehat{\mathbf{\Sigma}} : \nabla_{\hat{\mathbf{x}}}\widehat{\mathbf{w}}^S \, d\hat{\mathbf{x}} \\
&\quad = \int_{\widehat{\Omega}^S} \rho^{S,n}\mathbf{g} \cdot \widehat{\mathbf{w}}^S \, d\hat{\mathbf{x}} + \int_{\Gamma_0} \mathbf{F}^{n+1}\mathbf{\Sigma}^{n+1}\mathbf{N}^S \cdot \mathbf{W}^S \, dS
\end{aligned} \tag{23}$$

for all $\widehat{\mathbf{w}}^S : \widehat{\Omega}^S \to \mathbb{R}^2$, $\widehat{\mathbf{w}}^S = 0$ on Γ_0^D. We recall that the forces $\mathbf{F}^{n+1}\mathbf{\Sigma}^{n+1}\mathbf{N}^S$ on the interface Γ_0 are assumed known.

From [21], chapter 3.2, if $\mathbf{A}$ is a square matrix, by linearization, we have:

$$\det(\mathbf{I} + \mathbf{A}) \approx 1 + tr(\mathbf{A}), \quad (\mathbf{I} + \mathbf{A})^{-1} \approx \mathbf{I} - \mathbf{A}, \quad \ln(1 + x) \approx x.$$

From (21) and because $\Delta t \nabla_{\hat{\mathbf{x}}}\widehat{\mathbf{v}}^{S,n+1}$ is small, we can approach $\widehat{\mathbf{F}}^{-1}$ by $\mathbf{I} - \Delta t \nabla_{\hat{\mathbf{x}}}\widehat{\mathbf{v}}^{S,n+1}$ and $\ln \widehat{J}$ by $(\Delta t) tr(\nabla_{\hat{\mathbf{x}}}\widehat{\mathbf{v}}^{S,n+1})$.

Now, we linearize the map

$$\widehat{\mathbf{v}}^{S,n+1} \to \widehat{\mathbf{F}}\widehat{\mathbf{\Sigma}} = \frac{\lambda^S}{J^n}(\ln J^n + \ln \widehat{J})\widehat{\mathbf{F}}^{-T} + \frac{\mu^S}{J^n}\left(\widehat{\mathbf{F}}\mathbf{F}^n(\mathbf{F}^n)^T - \widehat{\mathbf{F}}^{-T}\right) \tag{24}$$

by

$$\begin{aligned}
\widehat{\mathbf{L}}\left(\widehat{\mathbf{v}}^{S,n+1}\right) &= \frac{\lambda^S}{J^n}\ln J^n\left(\mathbf{I} - \Delta t\left(\nabla_{\hat{\mathbf{x}}}\widehat{\mathbf{v}}^{S,n+1}\right)^T\right) + \frac{\lambda^S}{J^n}(\Delta t) tr(\nabla_{\hat{\mathbf{x}}}\widehat{\mathbf{v}}^{S,n+1})\mathbf{I} \\
&\quad + \frac{\mu^S}{J^n}\left(\left(\mathbf{I} + \Delta t \nabla_{\hat{\mathbf{x}}}\widehat{\mathbf{v}}^{S,n+1}\right)\mathbf{F}^n(\mathbf{F}^n)^T - \mathbf{I} + \Delta t\left(\nabla_{\hat{\mathbf{x}}}\widehat{\mathbf{v}}^{S,n+1}\right)^T\right).
\end{aligned} \tag{25}$$

The linearized updated Lagrangian weak formulation of the structure is knowing $\mathbf{U}^{S,n} : \Omega_0^S \to \mathbb{R}^2$, $\widehat{\Omega}^S = \Omega_n^S$ and $\mathbf{v}^{S,n} : \widehat{\Omega}^S \to \mathbb{R}^2$, find $\widehat{\mathbf{v}}^{S,n+1} : \widehat{\Omega}^S \to \mathbb{R}^2$, $\widehat{\mathbf{v}}^{S,n+1} = 0$ on Γ_0^D such that

DOI: 10.1002/nme

$$\begin{aligned}\int_{\widehat{\Omega}^S} \rho^{S,n} \frac{\widehat{\mathbf{v}}^{S,n+1} - \mathbf{v}^{S,n}}{\Delta t} \cdot \widehat{\mathbf{w}}^S \, d\hat{\mathbf{x}} + \int_{\widehat{\Omega}^S} \widehat{\mathbf{L}}\left(\widehat{\mathbf{v}}^{S,n+1}\right) : \nabla_{\hat{\mathbf{x}}} \widehat{\mathbf{w}}^S \, d\hat{\mathbf{x}} \\ = \int_{\widehat{\Omega}^S} \rho^{S,n} \mathbf{g} \cdot \widehat{\mathbf{w}}^S \, d\hat{\mathbf{x}} + \int_{\Gamma_0} \mathbf{F}^{n+1} \boldsymbol{\Sigma}^{n+1} \mathbf{N}^S \cdot \mathbf{W}^S \, dS\end{aligned} \tag{26}$$

for all $\widehat{\mathbf{w}}^S : \widehat{\Omega}^S \to \mathbb{R}^2$, $\widehat{\mathbf{w}}^S = 0$ on Γ_0^D.

In view of (25), in order to compute the stiffness matrix in the aforementioned equation, we have to integrate $\mathbf{F}^n$ over $\widehat{\Omega}^S$. We use the convention that $\mathbf{F}^n(\mathbf{X}) = \widehat{G}(\hat{\mathbf{x}})$ where $\hat{\mathbf{x}} = \mathbf{X} + \mathbf{U}^{S,n}(\mathbf{X})$.

We put

$$\mathbf{U}^{S,n+1}(\mathbf{X}) = \mathbf{U}^{S,n}(\mathbf{X}) + \Delta t \, \widehat{\mathbf{v}}^{S,n+1}(\hat{\mathbf{x}}) \tag{27}$$

and we can get the new structure domain Ω_{n+1}^S as the image of $\widehat{\Omega}^S$ via the map

$$\hat{\mathbf{x}} \to \mathbf{x} = \hat{\mathbf{x}} + \Delta t \, \widehat{\mathbf{v}}^{S,n+1}(\hat{\mathbf{x}}) \tag{28}$$

then set $\mathbf{v}^{S,n+1} : \Omega_{n+1}^S \to \mathbb{R}^2$ as follows

$$\mathbf{v}^{S,n+1}(\mathbf{x}) = \widehat{\mathbf{v}}^{S,n+1}(\hat{\mathbf{x}}). \tag{29}$$

The time advancing scheme for structural equations is given by (26)–(29).

5. ARBITRARY LAGRANGIAN–EULERIAN FRAMEWORK FOR APPROXIMATION OF FLUID EQUATIONS

The Arbitrary Lagrangian–Eulerian (ALE) framework is a successful method to solve fluid equations in moving domain [24]. Let $\widehat{\Omega}^F$ be a reference fluid domain, and let $\mathcal{A}_t$, $t \in [0, T]$ be a family of transformations such that: $\mathcal{A}_t(\hat{\mathbf{x}}) = \hat{\mathbf{x}}$ for all $\hat{\mathbf{x}} \in \Sigma_1 \cup \Sigma_2 \cup \Sigma_3$ and $\mathcal{A}_t(\widehat{\Omega}^F) = \Omega_t^F$, where $\hat{\mathbf{x}} = (\widehat{x}_1, \widehat{x}_2)^T \in \widehat{\Omega}^F$ are the ALE coordinates and $\mathbf{x} = (x_1, x_2)^T = \mathcal{A}_t(\hat{\mathbf{x}})$ the Eulerian coordinates.

Let $\mathbf{v}^F$ be the fluid velocity in the Eulerian coordinates. We denote by $\widehat{\mathbf{v}}^F : \widehat{\Omega}^F \to \mathbb{R}^2$ the corresponding function in the ALE coordinates, which is defined by $\widehat{\mathbf{v}}^F(\hat{\mathbf{x}}, t) = \mathbf{v}^F(\mathcal{A}_t(\hat{\mathbf{x}}), t) = \mathbf{v}^F(\mathbf{x}, t)$. We denote the mesh velocity by $\boldsymbol{\vartheta}(\mathbf{x}, t) = \frac{\partial \mathcal{A}_t}{\partial t}(\hat{\mathbf{x}}) = \frac{\partial \mathcal{A}_t}{\partial t}(\mathcal{A}_t^{-1}(\mathbf{x}))$ and the ALE time derivative of the fluid velocity by $\left.\frac{\partial \mathbf{v}^F}{\partial t}\right|_{\hat{\mathbf{x}}}(\mathbf{x}, t) = \frac{\partial \widehat{\mathbf{v}}^F}{\partial t}(\hat{\mathbf{x}}, t)$.

The Navier–Stokes equations in the ALE framework give:

$$\begin{aligned}\rho^F \left(\left.\frac{\partial \mathbf{v}^F}{\partial t}\right|_{\hat{\mathbf{x}}} + \left(\left(\mathbf{v}^F - \boldsymbol{\vartheta}\right) \cdot \nabla\right) \mathbf{v}^F \right) - 2\mu^F \nabla \cdot \epsilon\left(\mathbf{v}^F\right) + \nabla p^F = \rho^F \mathbf{g}, \quad \text{in } \Omega_t^F \times (0, T) \\ \nabla \cdot \mathbf{v}^F = 0, \quad \text{in } \Omega_t^F \times (0, T)\end{aligned}$$

We denote by $\mathbf{v}^{F,n}$, $p^{F,n}$, the approximations of $\mathbf{v}^F(\cdot, t_n)$, $p^F(\cdot, t_n)$, respectively.

We set $\widehat{\Omega}^F = \Omega_n^F$ and we define $\boldsymbol{\vartheta}^n = \left(\vartheta_1^n, \vartheta_2^n\right)^T$ the velocity of the fluid domain as solution of

$$\begin{cases} \Delta_{\hat{\mathbf{x}}} \boldsymbol{\vartheta}^n = 0, & \Omega_n^F \\ \boldsymbol{\vartheta}^n = 0, & \partial\Omega_n^F \setminus \Gamma_n \\ \boldsymbol{\vartheta}^n = \mathbf{v}^{F,n}, & \Gamma_n. \end{cases} \tag{30}$$

For all $n = 0, \cdots, N-1$, we denote by $\mathcal{A}_{t_{n+1}}$ the map from $\overline{\Omega}_n^F$ to $\mathbb{R}^2$ defined by $\mathcal{A}_{t_{n+1}}(\widehat{x}_1, \widehat{x}_2) = (\widehat{x}_1 + \Delta t \vartheta_1^n, \widehat{x}_2 + \Delta t \vartheta_2^n)$. We set $\Omega_{n+1}^F = \mathcal{A}_{t_{n+1}}(\Omega_n^F)$, $\Gamma_{n+1} = \mathcal{A}_{t_{n+1}}(\Gamma_n)$ and we remark that $\hat{\mathbf{x}} = \mathcal{A}_{t_{n+1}}(\hat{\mathbf{x}})$, for all $\hat{\mathbf{x}} \in \Sigma_1 \cup \Sigma_2 \cup \Sigma_3$.

We define the fluid velocity $\widehat{\mathbf{v}}^{F,n+1} : \Omega_n^F \to \mathbb{R}^2$ and the fluid pressure $\widehat{p}^{F,n+1} : \Omega_n^F \to \mathbb{R}$ by

$$\widehat{\mathbf{v}}^{F,n+1}(\hat{\mathbf{x}}) = \mathbf{v}^{F,n+1}(\mathbf{x}), \quad \widehat{p}^{F,n+1}(\hat{\mathbf{x}}) = p^{F,n+1}(\mathbf{x}), \quad \forall \hat{\mathbf{x}} \in \Omega_n^F, \, \mathbf{x} = \mathcal{A}_{t_{n+1}}(\hat{\mathbf{x}}) \in \Omega_{n+1}^F.$$

DOI: 10.1002/nme

The time advancing scheme for fluid equations is find $\widehat{\mathbf{v}}^{F,n+1} : \Omega_n^F \to \mathbb{R}^2$ and $\widehat{p}^{F,n+1} : \Omega_n^F \to \mathbb{R}$ such that

$$\rho^F \left(\frac{\widehat{\mathbf{v}}^{F,n+1} - \mathbf{v}^{F,n}}{\Delta t} + \left(\left(\mathbf{v}^{F,n} - \boldsymbol{\vartheta}^n \right) \cdot \nabla_{\hat{\mathbf{x}}} \right) \widehat{\mathbf{v}}^{F,n+1} \right) - 2\mu^F \nabla_{\hat{\mathbf{x}}} \cdot \epsilon \left(\widehat{\mathbf{v}}^{F,n+1} \right) + \nabla_{\hat{\mathbf{x}}} \widehat{p}^{F,n+1} = \rho^F \mathbf{g}, \text{ in } \Omega_n^F \tag{31}$$

$$\nabla_{\hat{\mathbf{x}}} \cdot \widehat{\mathbf{v}}^{F,n+1} = 0, \text{ in } \Omega_n^F \tag{32}$$

$$\sigma^F \left(\widehat{\mathbf{v}}^{F,n+1}, \widehat{p}^{F,n+1} \right) \mathbf{n}^F = \mathbf{h}_{in}^{n+1}, \text{ on } \Sigma_1 \tag{33}$$

$$\sigma^F \left(\widehat{\mathbf{v}}^{F,n+1}, \widehat{p}^{F,n+1} \right) \mathbf{n}^F = \mathbf{h}_{out}^{n+1}, \text{ on } \Sigma_3 \tag{34}$$

$$\widehat{\mathbf{v}}^{F,n+1} = 0, \text{ on } \Sigma_2 \tag{35}$$

The aforementioned time discretization scheme is based on the backward Euler scheme and a linearization of the convective term.

We multiply the Equations (31) by a test function $\widehat{\mathbf{w}}^F : \Omega_n^F \to \mathbb{R}^2$ such that $\widehat{\mathbf{w}}^F = 0$ on Σ_2 and the Equation (32) by a test function $\widehat{q} : \Omega_n^F \to \mathbb{R}$. After integrating them over the domain Ω_n^F and using the Green's formula and the corresponding boundary conditions, we obtain the following discrete weak form.

Find $\widehat{\mathbf{v}}^{F,n+1} : \Omega_n^F \to \mathbb{R}^2$ such that $\widehat{\mathbf{v}}^{F,n+1} = 0$ on Σ_2 and $\widehat{p}^{F,n+1} : \Omega_n^F \to \mathbb{R}$ such that

$$\begin{aligned} &\int_{\Omega_n^F} \rho^F \frac{\widehat{\mathbf{v}}^{F,n+1}}{\Delta t} \cdot \widehat{\mathbf{w}}^F \, d\hat{\mathbf{x}} + \int_{\Omega_n^F} \rho^F \left(\left(\left(\mathbf{v}^{F,n} - \boldsymbol{\vartheta}^n \right) \cdot \nabla_{\hat{\mathbf{x}}} \right) \widehat{\mathbf{v}}^{F,n+1} \right) \cdot \widehat{\mathbf{w}}^F \, d\hat{\mathbf{x}} \\ &\quad - \int_{\Omega_n^F} \left(\nabla_{\hat{\mathbf{x}}} \cdot \widehat{\mathbf{w}}^F \right) \widehat{p}^{F,n+1} d\hat{\mathbf{x}} + \int_{\Omega_n^F} 2\mu^F \epsilon \left(\widehat{\mathbf{v}}^{F,n+1} \right) : \epsilon \left(\widehat{\mathbf{w}}^F \right) d\hat{\mathbf{x}} \\ &= \mathcal{L}_F(\widehat{\mathbf{w}}^F) + \int_{\Gamma_n} \left(\sigma^F \left(\widehat{\mathbf{v}}^{F,n+1}, \widehat{p}^{F,n+1} \right) \mathbf{n}^F \right) \cdot \widehat{\mathbf{w}}^F \, ds, \end{aligned} \tag{36}$$

$$\int_{\Omega_n^F} \left(\nabla_{\hat{\mathbf{x}}} \cdot \widehat{\mathbf{v}}^{F,n+1} \right) \widehat{q} \, d\hat{\mathbf{x}} = 0, \tag{37}$$

for all $\widehat{\mathbf{w}}^F : \Omega_n^F \to \mathbb{R}^2$ such that $\widehat{\mathbf{w}}^F = 0$ on Σ_2 and for all $\widehat{q} : \Omega_n^F \to \mathbb{R}$, where

$$\mathcal{L}_F \left(\widehat{\mathbf{w}}^F \right) = \int_{\Omega_n^F} \rho^F \frac{\widehat{\mathbf{v}}^{F,n}}{\Delta t} \cdot \widehat{\mathbf{w}}^F \, d\hat{\mathbf{x}} + \int_{\Omega_n^F} \rho^F \mathbf{g} \cdot \widehat{\mathbf{w}}^F + \int_{\Sigma_1} \mathbf{h}_{in}^{n+1} \cdot \widehat{\mathbf{w}}^F + \int_{\Sigma_3} \mathbf{h}_{out}^{n+1} \cdot \widehat{\mathbf{w}}^F.$$

6. MONOLITHIC FORMULATION FOR THE FLUID–STRUCTURE EQUATIONS

We will denote $\Omega_n = \Omega_n^F \cup \Gamma_n \cup \Omega_n^S$ and let us introduce the global velocity, pressure, and test function

$$\widehat{\mathbf{v}}^{n+1} : \Omega_n \to \mathbb{R}^2, \quad \widehat{p}^{n+1} : \Omega_n \to \mathbb{R}, \quad \widehat{\mathbf{w}} : \Omega_n \to \mathbb{R}^2$$

$$\widehat{\mathbf{v}}^{n+1} = \begin{cases} \widehat{\mathbf{v}}^{F,n+1} \text{ in } \Omega_n^F \\ \widehat{\mathbf{v}}^{S,n+1} \text{ in } \Omega_n^S \end{cases} \quad \widehat{p}^{n+1} = \begin{cases} \widehat{p}^{F,n+1} \text{ in } \Omega_n^F \\ \widehat{p}^{S,n+1} \text{ in } \Omega_n^S \end{cases} \quad \widehat{\mathbf{w}} = \begin{cases} \widehat{\mathbf{w}}^F \text{ in } \Omega_n^F \\ \widehat{\mathbf{w}}^S \text{ in } \Omega_n^S. \end{cases}$$

DOI: 10.1002/nme

At each time step, we solve the linear coupled problem: find $\widehat{\mathbf{v}}^{n+1} \in \left(H^1(\Omega_n)\right)^2$, $\widehat{\mathbf{v}}^{n+1} = 0$ on $\Sigma_2 \cup \Gamma_0^D$ and $\widehat{p}^{n+1} \in L^2(\Omega_n)$, $\widehat{p}^{n+1} = 0$ in Ω_n^S, such that

$$\begin{aligned}
&\int_{\Omega_n^F} \rho^F \frac{\widehat{\mathbf{v}}^{n+1}}{\Delta t} \cdot \widehat{\mathbf{w}} d\hat{\mathbf{x}} + \int_{\Omega_n^F} \rho^F \left(\left((\mathbf{v}^n - \boldsymbol{\vartheta}^n) \cdot \nabla_{\hat{\mathbf{x}}}\right) \widehat{\mathbf{v}}^{n+1}\right) \cdot \widehat{\mathbf{w}} d\hat{\mathbf{x}} \\
&\quad - \int_{\Omega_n^F} \left(\nabla_{\hat{\mathbf{x}}} \cdot \widehat{\mathbf{w}}\right) \widehat{p}^{n+1} d\hat{\mathbf{x}} + \int_{\Omega_n^F} 2\mu^F \epsilon\left(\widehat{\mathbf{v}}^{n+1}\right) : \epsilon\left(\widehat{\mathbf{w}}\right) d\hat{\mathbf{x}} \\
&\quad + \int_{\Omega_n^S} \rho^{S,n} \frac{\widehat{\mathbf{v}}^{n+1}}{\Delta t} \cdot \widehat{\mathbf{w}}\, d\hat{\mathbf{x}} + \int_{\Omega_n^S} \widehat{\mathbf{L}}\left(\widehat{\mathbf{v}}^{n+1}\right) : \nabla_{\hat{\mathbf{x}}} \widehat{\mathbf{w}}\, d\hat{\mathbf{x}} \\
&= \mathcal{L}_F(\widehat{\mathbf{w}}) + \int_{\Omega_n^S} \rho^{S,n} \frac{\mathbf{v}^n}{\Delta t} \cdot \widehat{\mathbf{w}}\, d\hat{\mathbf{x}} + \int_{\Omega_n^S} \rho^{S,n} \mathbf{g} \cdot \widehat{\mathbf{w}}\, d\hat{\mathbf{x}},
\end{aligned} \tag{38}$$

$$\int_{\Omega_n^F} \left(\nabla_{\hat{\mathbf{x}}} \cdot \widehat{\mathbf{v}}^{n+1}\right) \widehat{q}\, d\hat{\mathbf{x}} = 0, \tag{39}$$

for all $\widehat{\mathbf{w}} \in \left(H^1(\Omega_n)\right)^2$, $\widehat{\mathbf{w}} = 0$ on $\Sigma_2 \cup \Gamma_0^D$ and for all $\widehat{q} \in L^2(\Omega_n)$.

Remark 1

(i) Because $\widehat{\mathbf{v}}^{n+1} \in \left(H^1(\Omega_n)\right)^2$, then the traces of $\widehat{\mathbf{v}}^{F,n+1}$ and $\widehat{\mathbf{v}}^{S,n+1}$ on Γ_n are well defined and

$$\widehat{\mathbf{v}}^{F,n+1}_{|\Gamma_n} = \widehat{\mathbf{v}}^{S,n+1}_{|\Gamma_n}$$

which is a discrete form of the continuity of the velocity at the interface (9).

(ii) If the solution of (38)–(39) is smooth, from (38), (26), and (36), we obtain

$$\begin{aligned}
\int_{\Gamma_0} \mathbf{F}^{n+1} \boldsymbol{\Sigma}^{n+1} \mathbf{N}^S \cdot \mathbf{W}^S\, dS &= -\int_{\Gamma_n} \left(\sigma^F\left(\widehat{\mathbf{v}}^{F,n+1}, \widehat{p}^{F,n+1}\right) \mathbf{n}^F\right) \cdot \widehat{\mathbf{w}}^F\, ds \\
&= -\int_{\Gamma_0} \omega^n \left(\sigma^F\left(\widehat{\mathbf{v}}^{F,n+1}, \widehat{p}^{F,n+1}\right) \mathbf{n}^F\right)_{\left(Id + \mathbf{U}^{S,n}\right)} \cdot \mathbf{W}^F\, dS
\end{aligned}$$

where $\omega^n = \left\|\text{cof}\ \left(\mathbf{F}^n\right) \mathbf{N}^S\right\|_{\mathbb{R}^2}$. But $\widehat{\mathbf{w}} \in \left(H^1(\Omega_n)\right)^2$, then the traces on Γ_n are well defined and $\widehat{\mathbf{w}}^F_{|\Gamma_n} = \widehat{\mathbf{w}}^S_{|\Gamma_n}$, which gives $\mathbf{W}^F_{|\Gamma_0} = \mathbf{W}^S_{|\Gamma_0}$. Because $\widehat{\mathbf{w}}$ is arbitrary, we obtain

$$\mathbf{F}^{n+1} \boldsymbol{\Sigma}^{n+1} \mathbf{N}^S = -\omega^n \left(\sigma^F\left(\widehat{\mathbf{v}}^{F,n+1}, \widehat{p}^{F,n+1}\right) \mathbf{n}^F\right)_{\left(Id + \mathbf{U}^{S,n}\right)}, \quad \text{almost everywhere on } \Gamma_0$$

which is a discrete form of the continuity of the forces at the interface (10).

Algorithm for fluid–structure interaction Time advancing scheme from n to $n+1$
We assume that we know Ω_n, $\mathbf{v}^n$, p^n, $\boldsymbol{\vartheta}^n$.

Step 1: Solve the linear system (38)–(39) and obtain the velocity $\widehat{\mathbf{v}}^{n+1}$ and the pressure $\widehat{p}^{n+1}$.

Step 2: Compute the mesh velocity $\widehat{\boldsymbol{\vartheta}}^{n+1} \Omega_n \to \mathbb{R}^2$

$$\begin{cases}
\Delta_{\hat{\mathbf{x}}} \widehat{\boldsymbol{\vartheta}}^{n+1} = 0, & \Omega_n^F \\
\widehat{\boldsymbol{\vartheta}}^{n+1} = 0, & \partial\Omega_n^F \setminus \Gamma_n \\
\widehat{\boldsymbol{\vartheta}}^{n+1} = \widehat{\mathbf{v}}^{n+1}, & \Gamma_n.
\end{cases} \tag{40}$$

We can replace in (40), the Laplacian by the linear elasticity operator in order to improve the quality of the mesh.

DOI: 10.1002/nme

Step 3: Define the map $\mathbb{T}_n : \overline{\Omega}_n \to \mathbb{R}^2$ by

$$\mathbb{T}_n(\hat{\mathbf{x}}) = \hat{\mathbf{x}} + (\Delta t)\widehat{\boldsymbol{\vartheta}}^{n+1}(\hat{\mathbf{x}})\chi_{\Omega_n^F}(\hat{\mathbf{x}}) + (\Delta t)\widehat{\mathbf{v}}^{n+1}(\hat{\mathbf{x}})\chi_{\Omega_n^S}(\hat{\mathbf{x}})$$

where $\chi_{\Omega_n^F}$ and $\chi_{\Omega_n^S}$ are the characteristic functions of fluid and structure domains.

Step 4: We set $\Omega_{n+1} = \mathbb{T}_n(\Omega_n)$. We define $\mathbf{v}^{n+1} : \Omega_{n+1} \to \mathbb{R}^2$, $p^{n+1} : \Omega_{n+1} \to \mathbb{R}$ and $\boldsymbol{\vartheta}^{n+1} : \Omega_{n+1} \to \mathbb{R}^2$ by

$$\mathbf{v}^{n+1}(\mathbf{x}) = \widehat{\mathbf{v}}^{n+1}(\hat{\mathbf{x}}),\ p^{n+1}(\mathbf{x}) = \widehat{p}^{n+1}(\hat{\mathbf{x}}),\ \boldsymbol{\vartheta}^{n+1}(\mathbf{x}) = \widehat{\boldsymbol{\vartheta}}^{n+1}(\hat{\mathbf{x}}),\ \forall \hat{\mathbf{x}} \in \Omega_n \text{ and } \mathbf{x} = \mathbb{T}_n(\hat{\mathbf{x}}).$$

Remark 2
We solve the monolithic system (38)–(39) using globally continuous finite element for the velocity $\widehat{\mathbf{v}}^{n+1} \in \left(H^1(\Omega_n)\right)^2$ defined all over the fluid–structure global mesh. Then the both continuity conditions at the interface hold in the sense of Remark 1. For the global pressure $\widehat{p}^{n+1} \in L^2(\Omega_n)$, we have to impose $\widehat{p}^{n+1} = 0$ in Ω_n^S; more precisely, we impose $\widehat{p}^{n+1} = 0$ at each node of the structure sub-domain excepting the nodes on the interface Γ_n.

7. NUMERICAL RESULTS

The numerical tests have been produced using *FreeFem++* [25].

7.1. Test 1. Flow through a channel with a flexible wall

Physical parameters
The geometrical configuration is represented in Figure 1. The fluid occupies initially the rectangle $\Omega_0^F = [0, L]\times[0, H]$ of length $L = 6$ cm and height $H = 1$ cm. The viscosity of the fluid was taken to be $\mu^F = 0.035\frac{g}{cm\cdot s}$, its density $\rho^F = 1\frac{g}{cm^3}$. The thickness of the elastic wall is $h^S = 0.1$ cm, and the structure occupies initially the rectangle $\Omega_0^S = [0, L] \times [H, H + h^S]$. The others physical parameters of the structure are the Young modulus $E = 3\cdot 10^6\frac{g}{cm\cdot s^2}$, the Poisson ratio $\nu^S = 0.3$, the density $\rho_0^S = 1.1\ \frac{g}{cm^3}$. The Lamé parameters are computed by the formulas $\lambda^S = \frac{\nu^S E}{(1-2\nu^S)(1+\nu^S)}$ and $\mu^S = \frac{E}{2(1+\nu^S)}$.

For the volume force in fluid and structure, we put $\mathbf{g} = (0, 0)^T$. The prescribed boundary stress at the inlet $\Sigma_1 = \{0\} \times [0, H]$ is

$$\mathbf{h}_{in}(\mathbf{x}, t) = \begin{cases} \left(10^3(1 - \cos(2\pi t/0.025)), 0\right), & \mathbf{x} \in \Sigma_1, 0 \leqslant t \leqslant 0.025 \\ (0, 0), & \mathbf{x} \in \Sigma_1, 0.025 \leqslant t \leqslant T \end{cases}$$

and $\mathbf{h}_{out} = (0, 0)$ at the outlet $\Sigma_3 = \{L\} \times [0, H]$. On $\Sigma_2 = [0, L] \times \{0\}$, on a (8). The structure is fixed at the left and at the right sides, $[AB] = \{0\} \times [H, H + h^S]$, respectively, $[CD] = \{L\} \times [H, H + h^S]$. The remaining boundary conditions are (3), (9), and (10).

Initially, the fluid and the structure are at rest.

Numerical parameters We have chosen the following numerical parameters: $\Delta t = 0.001\, s$ the time step and $N = 100$ the number of time steps. We have used for the fluid and structure domains a unique global mesh of 6048 triangles and 3167 vertices, see Figure 2. The global fluid–structure mesh could be obtained by 'gluing' the fluid and structure meshes which are matching at the interface. Using *FreeFem++* [25], it is possible to construct a global fluid–structure mesh with an 'interior boundary', which is the fluid–structure interface. For the finite element approximation of the fluid–structure velocity, we have used the triangular finite element $\mathbb{P}_1 + bubble$, and we have employed for the pressure the finite element $\mathbb{P}_1$. The linear fluid–structure system is solved using the LU decomposition.

DOI: 10.1002/nme

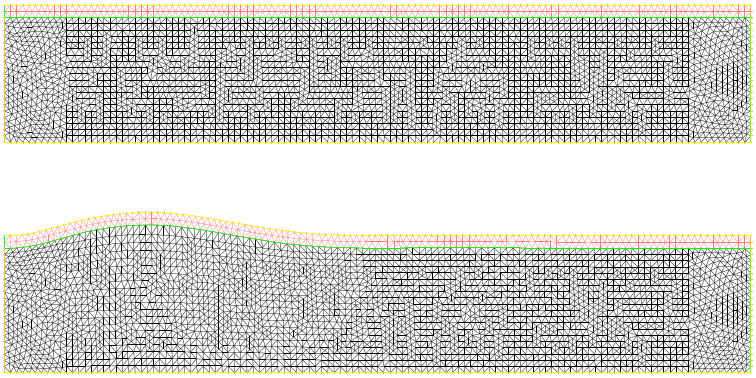

Figure 2. Test 1. Fluid–structure mesh at time instant $t = 0$ (top) and $t = 0.025$ (bottom).

CPU time The Test 1 was performed on a computer with a processor of 4 $\times$ 2.53 GHz frequency and 4 Go RAM. The CPU was 4min 13s using the monolithic approach. Using the partitioned procedures method described in [26], the CPU was 42min for $m = 3$, where m is the dimension of the optimization problem solved at each time step, in order to obtain the continuity of the stress at the fluid–structure interface. The optimization problem have been solved by the Broyden, Fletcher, Goldford, Shano (BFGS) algorithm. At each time step, the BFGS performs in average 6.96 iterations. At each BFGS iteration, 2.65 evaluations of the cost function are necessary in average for the line search and one call of the gradient. In this paper, we compute $\nabla J(\boldsymbol{\alpha})$ by the finite differences scheme

$$\frac{\partial J}{\partial \alpha_k}(\boldsymbol{\alpha}) \approx \frac{J(\boldsymbol{\alpha} + \Delta\alpha_k \mathbf{e_k}) - J(\boldsymbol{\alpha})}{\Delta\alpha_k}$$

where $\mathbf{e_k}$ is the kth vector of the canonical base of $\mathbb{R}^m$, and $\Delta\alpha_k = 10^{-6}$ is the grid spacing. Consequently, $m + 1 = 4$ calls of the cost function are needed in order to compute the gradient. To sum up, at each time step, the BFGS performs in average 46.31 evaluations of the cost function. Each cost function call consists in solving a linear fluid problem using the LU factorization and solving a non-linear structure problem using the Newton's method, which performs in average two iterations. The CPU was 1h 14min for $m = 5$ using the partitioned procedures method.

Behavior of the computed solution For $\Delta t = 0.001$ s, the fluid velocity and pressure at different time instants are plotted in Figures 3 and 4. A wave starts from the left side and goes to the right side. The pressure in the structure domain has no physical signification, and it is fixed to zero. The vertical displacements of three points at the interface for time steps $\Delta t = 0.001$ s, $\Delta t = 0.0005$ s, and $\Delta t = 0.0025$ s are presented in Figure 5 in the left column and for three mesh size $1/10$, $1/20$, $1/30$ in the right column. The time stability of the algorithm does not depend on the time step or the mesh size. We observe that the vertical displacements are less than 0.3 cm.

After $t = 0.025$ s, the prescribed boundary stress at the inlet $\mathbf{h}_{in}$ is $(0, 0)$, so the difference between the inlet stress at Σ_1 and the outlet stress at Σ_1 is zero. The system has a stored energy at the time instant $t = 0.025$ s, and it keeps on evolving afterwards, the vertical displacements of points at the interface are presented in Figure 5.

We can simulate a quasi-incompressible structure by using a large value for λ^S. In Figure 6, we can observe that the volume does not vary much for $\lambda^S = 10^8$.

7.2. Test 2. Flow around a flexible thin structure attached to a fixed cylinder

We have tested the benchmark FSI3 from [27].

The structure is composed by a rectangular flexible beam attached to a fixed circle. The circle center is positioned at $(0.2, 0.2)$ m measured from the left bottom corner of the channel. The circle

DOI: 10.1002/nme

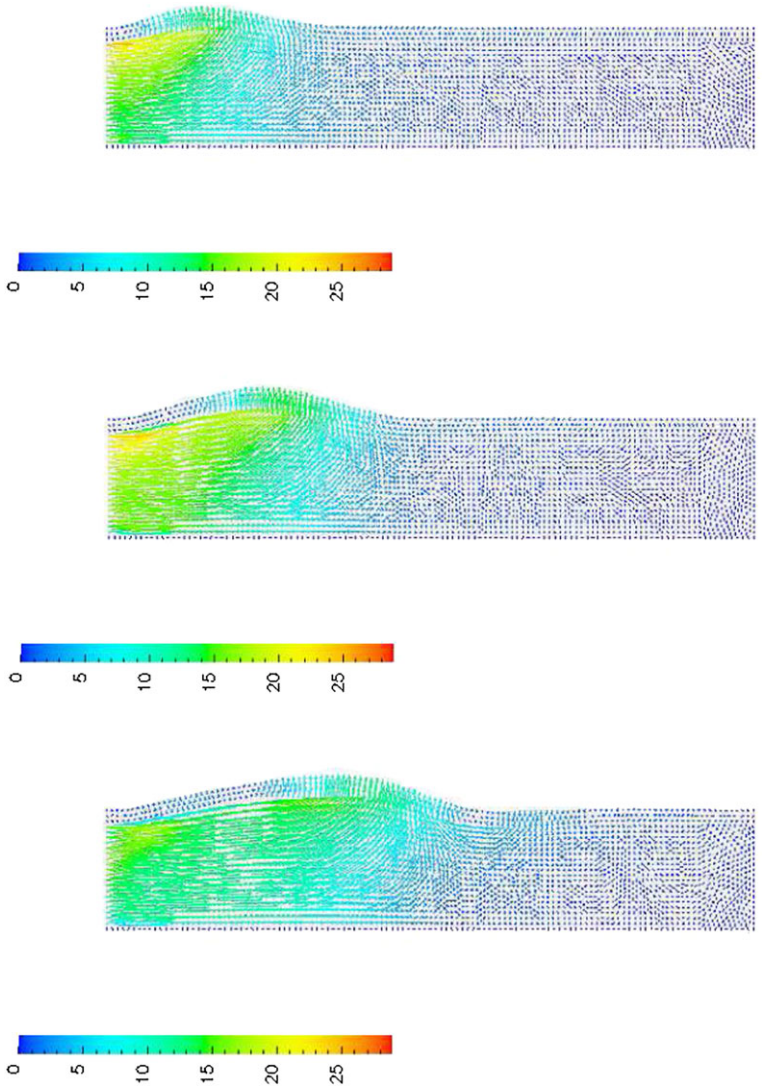

Figure 3. Test 1. Fluid–structure velocities [cm/s] at time instant $t = 0.015$ (top), $t = 0.025$ (middle), $t = 0.035$ (bottom).

has the radius $r = 0.5$ m and the rectangular beam is of length $\ell = 0.35$ m, thickness $h = 0.02$ m. The mass density is $\rho^S = 1000$ Kg/m^3, the Young modulus is $E^S = 5.6 \times 10^6$ Pa and the Poisson's ratio is $\nu^S = 0.4$.

The channel has the length $L = 2.5$ m and the width $H = 0.41$ m. The fluid dynamic viscosity is $\mu^F = 1$ Kg/(m s) and the mass density is $\rho^F = 1000$ Kg/m^3.

We denote by $\Sigma_1 = \{0\} \times [0, H]$, $\Sigma_3 = \{L\} \times [0, H]$ the left and the right vertical boundaries of the channel and by $\Sigma_2 = [0, L] \times \{0\}$, $\Sigma_4 = [0, L] \times \{H\}$ the bottom and the top boundaries, respectively.

We have used the boundary condition $\mathbf{v} = \mathbf{v}_{in}$ at the inflow Σ_1, where

$$\mathbf{v}_{in}(x_1, x_2, t) = \begin{cases} \left(1.5\,\overline{U}\,\frac{x_2(H-x_2)}{(H/2)^2}\,\frac{(1-\cos(\pi t/2))}{2}, 0\right), & (x_1, x_2) \in \Sigma_1, 0 \leqslant t \leqslant 2 \\ \left(1.5\,\overline{U}\,\frac{x_2(H-x_2)}{(H/2)^2}, 0\right), & (x_1, x_2) \in \Sigma_1, 2 \leqslant t \leqslant T = 10 \end{cases}$$

and $\overline{U} = 1.8$. At Σ_2, Σ_4, as well as on the boundary of the circle, we have imposed the no-slip boundary condition $\mathbf{v} = \mathbf{0}$. At the outflow Σ_3, we have imposed the traction free $\sigma^F(\mathbf{v}, p)\,\mathbf{n}^F = 0$.

Initially, the fluid and the structure are at rest.

DOI: 10.1002/nme

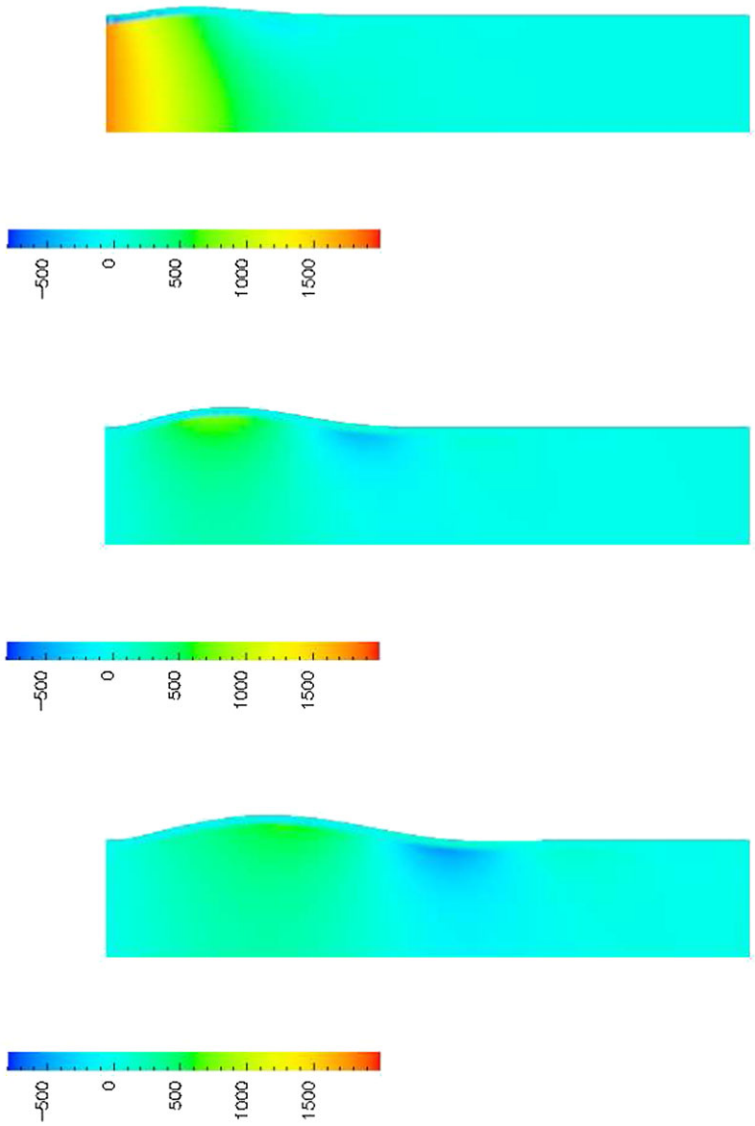

Figure 4. Test 1. Fluid–structure pressure [dynes/cm^2] at time instant $t = 0.015$ (top), $t = 0.025$ (middle), $t = 0.035$ (bottom).

We use a global mesh for the fluid–structure domain of 4964 triangles and 2604 vertices, see Figure 7 and the time step is $\Delta t = 0.002$ s. We have employed the same finite elements as for the Test 1.

After an initial transient period, the system settles into periodic large amplitude oscilations, Figure 8. We observe that the vertical displacements are less than 0.03 m. The average frequency in the time interval [8, 10] is about 5 Hz. We have used $\overline{U} = 1.8$ for the boundary condition at the inflow Σ_1 which is smaller that $\overline{U} = 2$ employed in [27] where the amplitude of the oscilations was about 0.034 m. The pressure in the structure domain has no physical signification, and it is fixed to zero, Figure 9, at the right.

7.3. Test 3. Flow around a slender flexible structure attached to a rigid square

This benchmark was proposed in [28] with the parameters 'Structure 2', used in [12], also. A rigid square is submerged in a fluid and a slender flexible structure is attached to the rigid body.

The square center is positioned at (5, 6) cm measured from the left bottom corner of the channel. The square is of the side length 1 cm, and the rectangular beam is of length $\ell = 4$ cm, thickness

DOI: 10.1002/nme

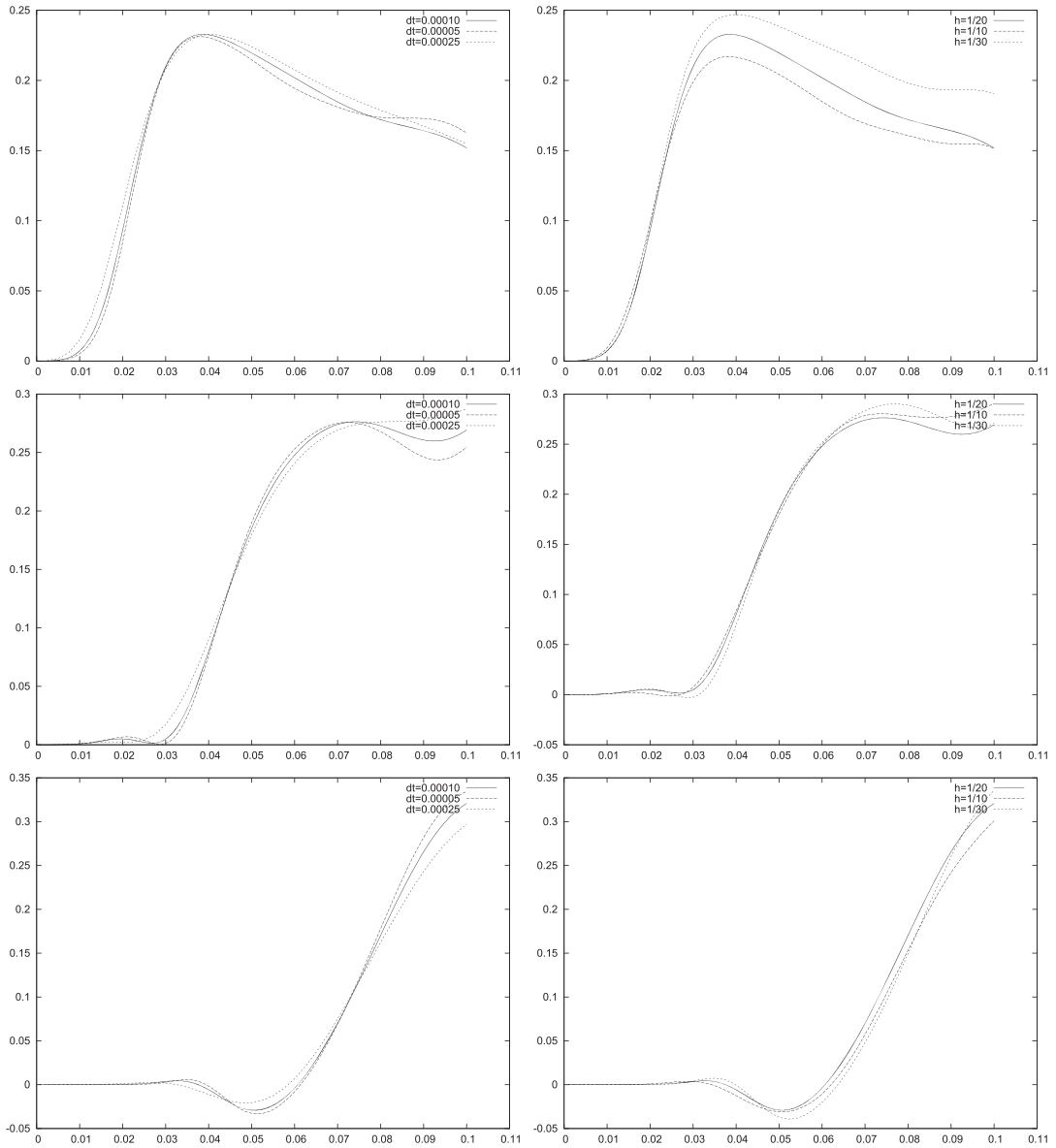

Figure 5. Test 1. Time history of the vertical displacement [cm] of three points on the interface when the left side of the structure is fixed. Points of horizontal coordinate $x_1 = \frac{L}{4}$ (top), $x_1 = \frac{L}{2}$ (middle), $x_1 = \frac{3L}{4}$ (bottom). We have used three time step $\Delta t = 0.001$, $\Delta t = 0.0005$, $\Delta t = 0.0025$ (left column) and three meshes of size $1/10$, $1/20$, $1/30$ (right column).

$h = 0.06$ cm. The mass density is $\rho^S = 2$ g/cm^3, the Young modulus is $E^S = 2 \times 10^6$(g/cm s) and the Poisson's ratio is $\nu^S = 0.35$.

The channel has the length $L = 19$ cm and the width $H = 12$ cm. The fluid dynamic viscosity is $\mu^F = 1.82 \times 10^{-4}$(g/cm s), and the mass density is $\rho^F = 1.18 \times 10^{-3}$g/cm^3.

We denote by $\Sigma_1 = \{0\} \times [0, H]$, $\Sigma_3 = \{L\} \times [0, H]$ the left and the right vertical boundaries of the channel and by $\Sigma_2 = [0, L] \times \{0\}$, $\Sigma_4 = [0, L] \times \{H\}$ the bottom and the top boundaries, respectively.

We have used the boundary condition $\mathbf{v} = (v_1, v_2) = (U^\infty, 0)$ at the inflow Σ_1, for $U^\infty = 25$ cm/s. 0n the boundary of the square, we have imposed the no-slip boundary condition $\mathbf{v} = \mathbf{0}$, at Σ_2 and Σ_4, $v_2 = 0$ and at the outflow Σ_3, we have imposed the traction free $\sigma^F(\mathbf{v}, p)\,\mathbf{n}^F = 0$.

Initially, the fluid and the structure are at rest.

DOI: 10.1002/nme

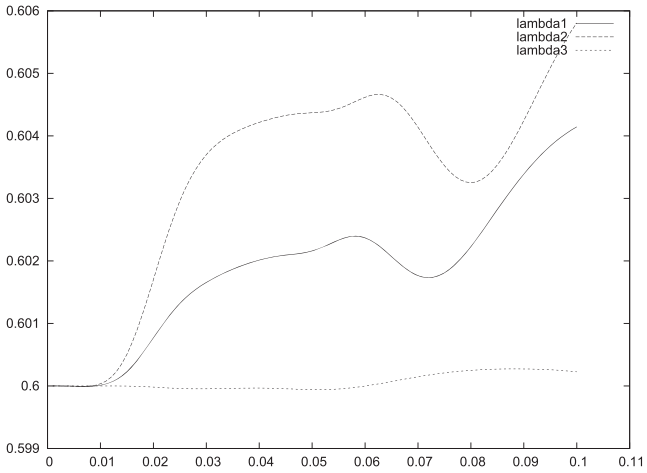

Figure 6. Test 1. The volume of the structure for $\lambda^S = \frac{\nu^S E}{(1-2\nu^S)(1+\nu^S)} = 1730769.23$, $\lambda^S = 0$ and $\lambda^S = 10^8$.

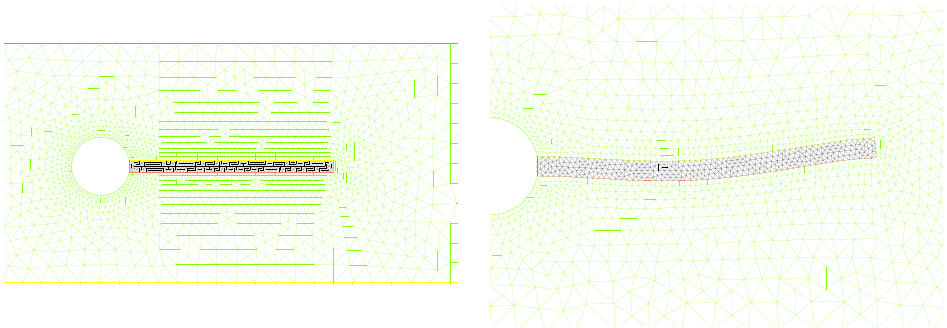

Figure 7. Test 2. Details of the fluid–structure mesh at $t = 0$ and $t = 8.732$.

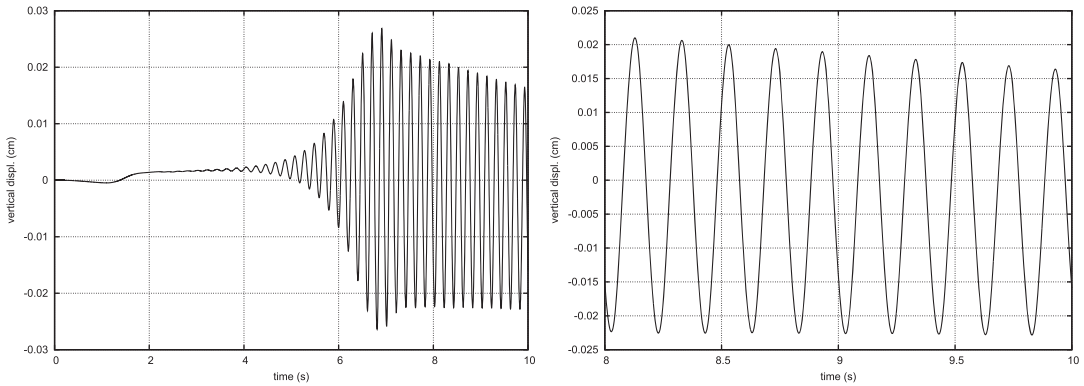

Figure 8. Test 2. Time history of the vertical displacement of the midle point of the left side of the structure.

We use a global mesh for the fluid–structure domain of 5107 triangles and 2625 vertices, see Figure 10 and the time step is $\Delta t = 0.001$ s. We have employed the same finite elements as for the Test 1.

We observe that the vertical displacements are less than 0.6 cm, see Figure 11. The average frequency in the time interval $[10, 15]$ is about 1.2 Hz. As in [28], several vortices developing in the vicinity of the deformed structure; see Figure 12 at the left. We have used $U^\infty = 25$ cm/s for the boundary condition at the inflow Σ_1 which is smaller that $\overline{U} = 51.3$ cm/s employed in [28] or

DOI: 10.1002/nme

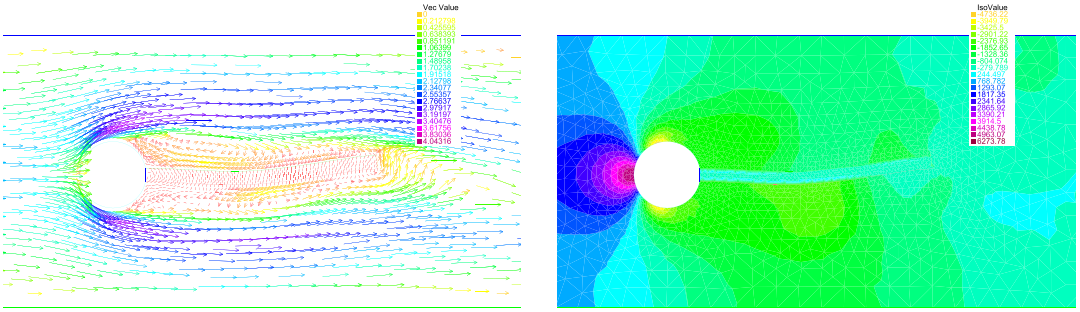

Figure 9. Test 2. Velocity and pressure at $t = 8.732$.

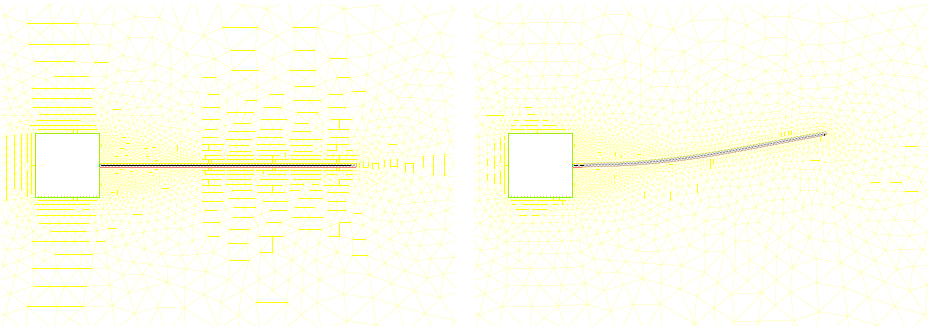

Figure 10. Test 3. Detail of the fluid–structure mesh at $t = 0$ and $t = 13.800$.

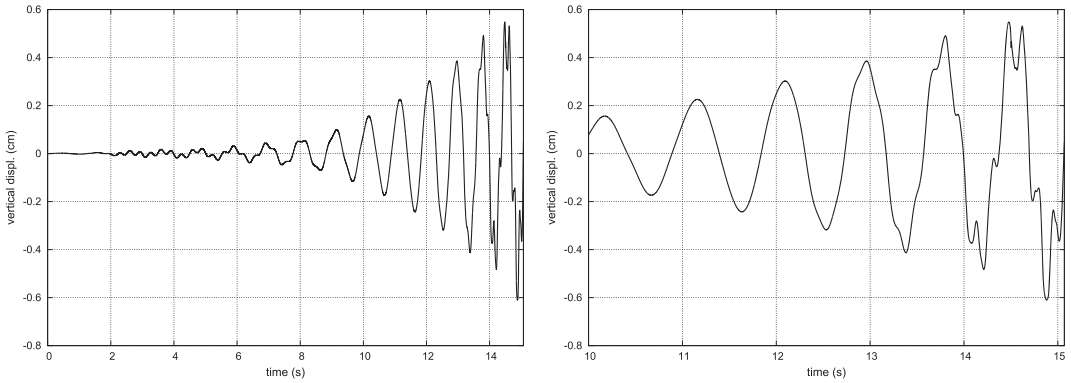

Figure 11. Test 3. Time history of the vertical displacement of the midle point of the left side of the structure.

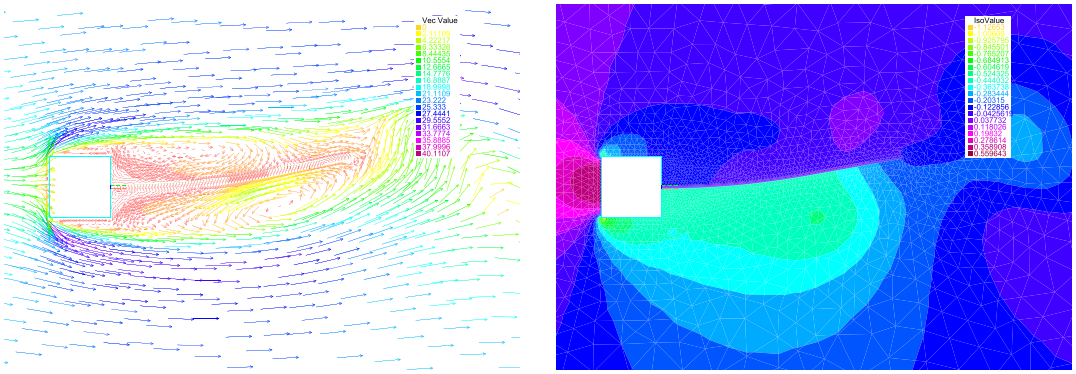

Figure 12. Test 3. Velocity and pressure at $t = 13.800$.

DOI: 10.1002/nme

$\overline{U} = 31.5$ cm/s employed in [12]. In the last cited paper, the maximum tip displacement is 0.8 cm with a frequency of 0.8 Hz. For $\overline{U} = 51.3$ or $\overline{U} = 31.5$, the rotation of the right side of the structure is important, and the construction of the ALE mesh using (40) fails.

8. CONCLUSIONS

We have used a global moving mesh for the fluid–structure domain, where the fluid–structure interface is an interior boundary of the global mesh. The continuity of velocity at the interface is automatically satisfied because we use continuous finite elements. The continuity of stress does not appear explicitly in the monolithic fluid–structure system, that we solve at each time step. The method is fast compared with a particular partitioned procedure algorithm.

REFERENCES

1. Formaggia L, Gerbeau GF, Nobile F, Quarteroni A. On the coupling of 3D and 1D Navier–Stokes equations for flow problems in compliant vessels. *Computer Methods in Applied Mechanics and Engineering* 2001; **191**:561–582.
2. Le Tallec P, Mouro J. Fluid structure interaction with large structural displacements. *Computer Methods in Applied Mechanics and Engineering* 2001; **190**:3039–3067.
3. Nobile F. Numerical approximation of fluid–structure interaction problems with application to haemodynamics. *Ph.D. Thesis*, EPFL, Switzerland, 2001.
4. Dettmer W, Perić D. A computational framework for fluid–structure interaction: finite element formulation and applications. *Computer Methods in Applied Mechanics and Engineering* 2006; **195**:5754–5779.
5. Fernàndez MA, Moubachir M. A Newton method using exact jacobians for solving fluid–structure coupling. *Computers & Structures* 2005; **83**:127–142.
6. Gerbeau GF, Vidrascu M. A quasi-Newton algorithm on a reduced model for fluid–structure interaction problems in blood flows. *Mathematical Modelling and Numerical Analysis* 2003; **37**:631–648.
7. Kuberry P, Lee H. A decoupling algorithm for fluid–structure interaction problems based on optimization. *Computer Methods in Applied Mechanics and Engineering* 2013; **267**:594–605.
8. Murea CM. Numerical simulation of a pulsatile flow through a flexible channel. *ESAIM Mathematical Modelling and Numerical Analysis* 2006; **40**:1101–1125.
9. Mbaye I, Murea CM. Numerical procedure with analytic derivative for unsteady fluid–structure interaction. *Communications in Numerical Methods in Engineering* 2008; **24**(11):1257–1275.
10. Dunne T. An Eulerian approach to fluid–structure interaction and goal-oriented mesh adaptation. *International Journal for Numerical Methods in Fluids* 2006; **51**:1017–1039.
11. Heil M, Hazed AL, Boyle J. Solvers for large-displacement fluid–structure interaction problems: segregated versus monolithic approaches. *Computer Mechanical* 2008; **193**:91–101.
12. Hubner B, Walhorn E, Dinkler D. A monolithic approach to fluid–structure interaction using space-time finite elements. *Computer Methods in Applied Mechanics and Engineering* 2004; **193**:2087–2104.
13. Hron J, Turek S. *A Monolithic FEM/multigrid Solver for an ALE Formulation of Fluid–Structure Interaction with Application in Biomechanics In Fluid-Structure Interaction*, Lect. Notes. Comput. Sci. Eng. 53. Springer: Berlin, 2006.
14. Badia S, Quaini A, Quarteroni A. Modular vs. non-modular preconditioners for fluid–structure systems with large added-mass effect. *Computer Methods in Applied Mechanics and Engineering* 2008; **197**(49-50):4216–4232.
15. Causin P, Gerbeau JF, Nobile F. Added-mass effect in the design of partitioned algorithms for fluid–structure problems. *Computer Methods in Applied Mechanics and Engineering* 2005; **194**(42-44):4506–4527.
16. Farhat C, Lesoinne M. Two effcient staggered algorithms for the serial and parallel solution of three-dimensional nonlinear transient aeroelastic problems. *Computer Methods in Applied Mechanics and Engineering* 2000; **182**: 499–515.
17. Felippa CA, Park KC, Farhat C. Partitioned analysis of coupled mechanical systems. *Computer Methods in Applied Mechanics and Engineering* 2001; **190**:3247–3270.
18. Nobile F, Vergara C. An effective fluid–structure intercation formulation for vascular dynamics by generalized Robin conditions. *SIAM Journal on Scientific Computing* 2008; **30**(2):731–763.
19. Dettmer W, Perić D. A new staggered scheme for fluid–structure interaction. *International Journal for Numerical Methods in Engineering* 2013; **93**:1–22.
20. Simo JC, Pister KS. Remarks on rate constitutive equations for finite deformation problems: Computational implications. *Computer Methods in Applied Mechanics and Engineering* 1984; **46**:201–215.
21. Bonet J, Wood RD. *Nonlinear Continuum Mechanics for Finite Element Analysis*. Cambridge University Press: Cambridge, 2008.
22. Holzapfel GA. *Nonlinear Solid Mechanics. A Continuum Approach for Engineering*. John Wiley & Sons Ltd.: Chichester, 2000.
23. Ciarlet PG. *Élasticité Tridimensionnelle*. Masson, 1986.

DOI: 10.1002/nme

24. Quarteroni A, Formaggia L. Mathematical modelling and numerical simulation of the cardiovascular system. In *Handbook of numerical analysis*, Vol. XII, Ciarlet PG (ed.). North-Holland: Amsterdam, 2004; 3–127.
25. Hecht F, New development in FreeFem++. *Journal of Numerical Mathematics* 2012; **20**(3-4):251–265.
26. Murea CM, Sy S. A fast method for solving fluid–structure interaction problems numerically. *International Journal for Numerical Methods in Fluids* 2009; **60**(10):1149–1172.
27. Turek S, Hron J. Proposal for numerical benchmarking of fluid–structure interaction between an elastic object and laminar incompressible flow. In *Fluid-Structure Interaction - Modelling, Simulation, Optimization*, vol. 53, Bungartz HJ, Schfer M (eds)., Lect. Notes Comput. Sci. Eng. Springer: Berlin, 2006; 371–385.
28. Wall W, Ramm E. Fluid-structure interaction based upon a stabilized (ALE) finite element method. In *Computational Mechanics. New Trends and Applications*, Idelsohn SR, Onate E, Dvorkin EN (eds). CIMNE: Barcelona, 1998; 1–20.

DOI: 10.1002/nme